Nanoscale

COMMUNICATION

View Article Online
View Journal | View Issue

Cite this: *Nanoscale*, 2016, **8**, 6994

Received 4th January 2016,
Accepted 7th March 2016

DOI: 10.1039/c6nr00046k

www.rsc.org/nanoscale

SiC_7 siligraphene: a novel donor material with extraordinary sunlight absorption†

Huilong Dong,[a] Liujiang Zhou,*[b] Thomas Frauenheim,[b] Tingjun Hou,[a] Shuit-Tong Lee[a] and Youyong Li*[a]

The SiC_7 siligraphene (g-SiC_7) is a novel 2D nanomaterial with a graphene-like structure. Based on theoretical calculations, we have systematically investigated the structure, stability, electronic and optical properties of g-SiC_7 siligraphene. The calculated results reveal that g-SiC_7 siligraphene is a semiconductor with a direct band gap of 1.13 eV, which can be easily tuned by applying biaxial strain or a perpendicular electric field. Such a g-SiC_7 siligraphene shows superior sunlight optical absorbance and is better than g-SiC_2 siligraphene and single-layer black phosphorus (phosphorene) in near infrared and visible photon ranges, thus holding great potential for photovoltaics applications as a light donor material.

The superior electronic and mechanical properties displayed in graphene have made it highly desirable for fabrication of optoelectronic devices.[1] However, it is well-known that the semimetallic nature of graphene (as well as its silicon counterpart silicene) significantly restricts its widespread applications due to the impossibility in turning off electrical conduction below a certain limit,[2] which makes the opening up and tuning of the band gap in graphene (or silicene) extremely necessary.[3–6] So far, graphene or graphene-like two-dimensional (2D) nanomaterials with medium range band gaps (*i.e.*, 1.0–2.0 eV) that are highly desirable for field effect transistors and solar cells are still practically difficult to realize.[7] Considering the good compatibility, silicon is widely used for the semiconducting of graphene.[8–12] Stimulated by the theoretical investigations and the experimental fabrication of single-layered SiC,[13,14] more attention has been devoted to the design of novel 2D silicon–carbon compounds.[15–19] Notably, the theoretical prediction and experimental observation of 2D g-SiC_2 siligraphene[7,20] have revealed that the incorporation of silicon into the graphene honeycomb lattice is an effective approach to obtain graphene-like nanomaterials with variable electronic and optical properties, and the obtained siligraphene has gained extensive scientific interest.[19,21,22]

Recently, Shi and co-workers reported the stability and electronic properties of 2D Si_xC_{1-x} ($0 < x < 1$) monolayers mixing carbon and silicon atoms.[18] They found that stoichiometry and bonding structure of the 2D Si–C monolayers can greatly affect the electronic properties. For example, with the same stoichiometry, pt-SiC_2 is metallic but g-SiC_2 is a semiconductor due to their different bonding structures.[7,15] From graphene to 2D-SiC, the band gap of siligraphene can vary in the range of 0–3 eV, independent of the increasing content of silicon.[18] Among them, g-SiC_2 has exhibited great potential as a novel donor material in excitonic solar cells.[7] And another siligraphene, g-SiC_3 can serve as a topological insulator (TI) superior to graphene.[21] Based on the previous investigations,[18,19] we find that a novel stable siligraphene g-SiC_7 also shows remarkable optoelectronic properties. The structure, stability, electronic and optical properties of g-SiC_7 have been exploited based on *ab initio* calculations. Such a g-SiC_7 siligraphene is a semiconductor with a direct band gap of 1.13 eV, and is superior in light absorbance, which makes it promising as a donor material for optical devices. The molecular structure, stability, electronic and optical properties are discussed in detail. It is believed that the g-SiC_7 siligraphene can serve as a novel 2D material for optoelectronic applications with great potential.

The geometry optimizations and electronic property calculations were carried out by the Vienna *ab initio* simulation package (VASP).[23,24] The projector-augmented-wave (PAW)[25] potentials were employed to describe the electron–ion interactions. The generalized gradient approximation parametrized by Perdew, Burke, and Ernzerhof (GG-PBE)[26] was chosen as the exchange–correlation functional. Due to the fact that the DFT functional significantly underestimates the band gap,[27] the screened exchange hybrid density functional by Heyd, Scuseria, and Ernzerhof (HSE06)[28,29] was also adopted to obtain more accurate band gap (E_g) values.

[a]*Institute of Functional Nano & Soft Materials (FUNSOM), Soochow University, Suzhou, Jiangsu 215123, China. E-mail: yyli@suda.edu.cn*
[b]*Bremen Center for Computational Material Science, Universität Bremen, Am Fallturm 1, 28359 Bremen, Germany. E-mail: liujiang86@gmail.com*

†Electronic supplementary information (ESI) available: Computational details on stability and optical absorbance calculations, the phonon dispersion of g-SiC7 siligraphene and snapshots of FPMD simulation. See DOI: 10.1039/c6nr00046k

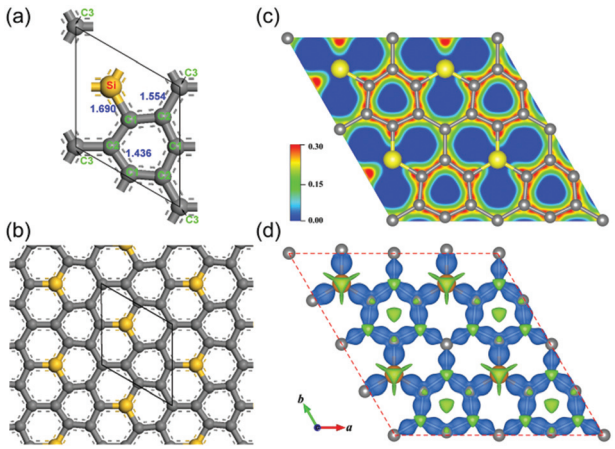

Fig. 1 (a) The optimized unit cell of g-SiC_7 siligraphene with the specific atomic composition (in green) and bond lengths (in blue). (b) The unit cell outlined as black lines in periodical structure. (c) The charge density projected on the g-SiC_7 siligraphene. (d) The charge density difference ($\Delta\rho$) of g-SiC_7 siligraphene. Isosurface value is set as 0.015 e A^{-3}; blue: $\Delta\rho > 0$, green: $\Delta\rho < 0$.

Table 1 Comparison of the symmetry, binding energy, band gaps, optical band gaps (E_g^{opt}), as well as exciton binding energy of graphene, silicene, single-layered SiC (SL-SiC) and the reported siligraphenes. The exciton binding energy is defined as the difference between the energy of the optical band gap and the quasiparticle band gap

	Symmetry group	Binding energy (eV per atom)	Band gap (eV)	E_g^{opt} (eV)	Exciton binding energy (eV)
Graphene	*P*3*m*1	8.66	0	NA	NA
g-SiC_7	*P*$\bar{6}$*m*2	7.07	0.76[a] 1.13[b] 1.55[c]	1.0	0.55
g-SiC_3	*P*6/*mmm*	6.70	0	NA	NA
g-SiC_2	*P*$\bar{6}$2*m*	6.46	0.60[a] 1.09[b] 1.38[c]	0.75	0.65[7]
SL-SiC	*P*$\bar{6}$*m*2	5.99	2.56[a] 2.90[b] 4.42[c]	3.25	1.17[37]
Silicene	*P*3*m*1	3.93	0	NA	NA

[a] Calculation results based on PBE. [b] Calculation results based on HSE06. [c] Calculation results based on G_0W_0. Data of g-SiC_2[7] and SL-SiC[37] are obtained from relevant references.

The unit cell of g-SiC_7 siligraphene (see Fig. 1a) belongs to the *P*$\bar{6}$*m*2 (no. 187) symmetry group, with the PBE-optimized a = 5.288 Å. All the atoms in g-SiC_7 siligraphene are strictly in-plane, without any buckling. As shown in Fig. 1b, there is one silicon atom and three different types of carbon atoms (named C1, C2 and C3) per unit cell. The silicon atom trigonally coordinates with the neighbouring carbon atoms (C1) with a Si–C distance of 1.69 Å and C–Si–C bond angle of 120°. The Si–C bond is significantly shorter than that in 2D-SiC (1.78–1.79 Å),[13,14] revealing a strong tendency for sp^2 hybridization. There is a hexagonal ring consisting of C1 and C2 atoms with a uniform bond length of 1.436 Å. However, unlike graphene, this hexagonal ring is not a regular hexagon, resulting from the different electronegative effects of Si and C3 atoms. Additionally, we calculated the total charge density and charge density difference of g-SiC_7 siligraphene to better analyse its structural characteristics, as displayed in Fig. 1c and d. The total charge density of g-SiC_7 siligraphene reveals a delocalized big π bonding in the 6 C-domain composed of C1 and C2 atoms. The Bader charge analysis[30,31] performed on g-SiC_7 indicates that Si atoms loses 2.61 |e| per atom, the C2 atoms lose 0.11 |e| per atom, while the C1 atoms obtain 0.92 |e| per atom and the C3 atoms obtain 0.20 |e| per atom. It is clear that the charge mainly transfers from Si to C1 atoms *via* the Si–C bonding interaction, and the central C3 atom derives less charge from C2 atoms, in accordance with Fig. 1d.

The stability of g-SiC_7 siligraphene has been confirmed in the previous work[18] [named (2, 0) structure according to its superlattice vector]. Here we performed more detailed calculations to verify it. First, the binding energy of g-SiC_7 siligraphene is calculated as 7.07 eV per atom, lower than that of graphene (8.66 eV per atom) but higher than the reported g-SiC_2 siligraphene (6.46 eV per atom)[7] and g-SiC_3 siligraphene (6.70 eV per atom)[19] (see Table 1). This is mainly due to the fact that the Si atom tends to adopt a sp^2–sp^3 hybridization to form the buckled pattern as silicene, which is greatly different from the pure sp^2 hybridization in graphene, leading to the phenomenon that the more Si atoms in planar siligraphene, the lower the stability. Then, the dynamical and thermal stability of g-SiC_7 siligraphene was also checked by phonon calculations and molecular dynamics, respectively. As shown in Fig. S1 of the ESI,† our calculated phonon dispersion exhibits no negative frequency, indicating that the g-SiC_7 siligraphene is dynamically stable. The snapshots of the g-SiC_7 supercell under different temperatures after 5 ps of the first principles molecular dynamics (FPMD) simulation are presented in Fig. S2.† The crystalline structure of g-SiC_7 siligraphene remains stable when the temperature is 2000 K and begins to decompose at a temperature of 3000 K. When the temperature rises to 3500 K, the crystalline totally deteriorates. Based on the FPMD results, the melting temperature of g-SiC_7 is estimated between 3000 K and 3500 K, indicating very high thermal stability, which is close to g-SiC_2 siligraphene (with a melting point of 3000–3500 K)[22] and is higher than pt-SiC_2 siligraphene (about 800–100 K).[15]

In addition, to check the elasticity of g-SiC_7 siligraphene, the elastic constants have been calculated. The calculation results generate c_{11} = 139.5 GPa and c_{12} = 43.5 GPa as independent elastic constants. In comparison, the calculated elastic constants of SL-SiC are c_{11} = 89.5 GPa and c_{12} = 26.4 GPa. Considering that the SiC NTs have been intensively investigated[32–34] and experimentally prepared already,[35,36] the larger elastic constants guarantee the feasibility that g-SiC_7 siligraphene can even be rolled into nanotubes.

Although its atomic composition is close to graphene, g-SiC_7 siligraphene is a semiconductor with a direct band gap (E_g) of 0.76 eV (PBE) or 1.13 eV (HSE06), thus holding great

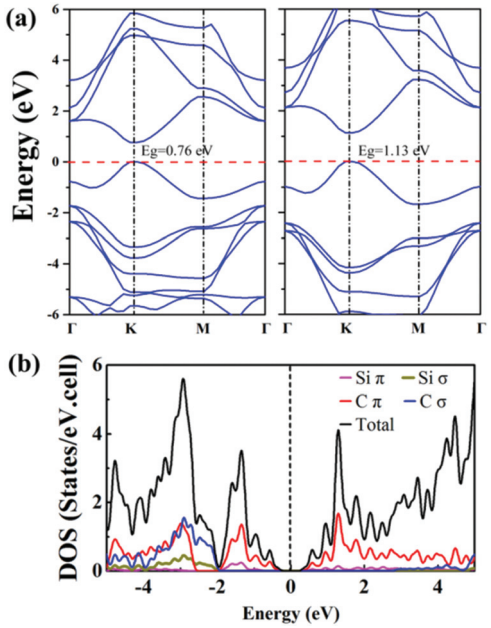

Fig. 2 (a) Band structure of g-SiC_7 siligraphene based on GGA-PBE (left panel) & HSE06 (right panel) calculations, respectively. Fermi level is set as zero. (b) Projected density of states (PDOS) of g-SiC_7 siligraphene.

potential for optoelectronic and transistor applications.[38] The band structure displayed in Fig. 2a indicates that both the valence band maximum (VBM) and conduction band minimum (CBM) locate at the *K* point, showing a preferable efficiency of light absorption. Near the Fermi level, there are two separated bands consisting of hybridized π and π* orbitals from Si and C atoms, which can be verified by the projected density of states (PDOS) (Fig. 2b). It has been suggested that the broken symmetry induced by the Si doping is responsible for the opening up of the band gap in g-SiC_7.[18] As we can see in Fig. 1b, due to the electronegativity and atomic radius difference between C and Si atoms, the introduction of Si atom into the plane leads to a much shorter bond length of C1–C2 (1.436 Å) than that of C2–C3 (1.554 Å), leading to a distortion in the honeycomb lattice. The electron density presented in Fig. 1c and d also implies a broken electron conjugation in g-SiC_7 siligraphene. For g-SiC_7, when all the carbon rings are marked out, there are still isolated C and Si atoms excluded from conjugated rings (Fig. 3a), which are not conjugated with each other and thus leading to the broken conjugation framework and the opening up of the band gap. In comparison, within the metallic g-SiC_3, whose CBM and VBM make contact with each other at the Fermi level, all the carbon and silicon atoms participate in the formation of the conjugation system consisting of C and Si rings (Fig. 3b), respectively. The synergetic conjugation between C and Si atoms guarantees the good conductance of electrons and enables g-SiC_3 to be a good conductor. So we can speculate that the broken conjugation is responsible for band gap opening in g-SiC_7 siligraphene, which helps in designing other siligraphenes with similar properties.

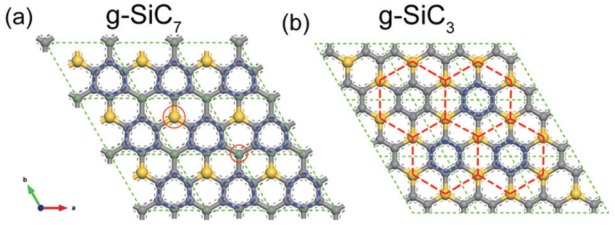

Fig. 3 Structural analysis of (a) g-SiC_7 and (b) g-SiC_3 3 × 3 supercells. The blue hexagonal rings mark the carbon rings and the red hexagonal rings mark the silicon rings. The isolated C and Si atoms excluded from conjugated carbon rings are indicated in red circles in (a).

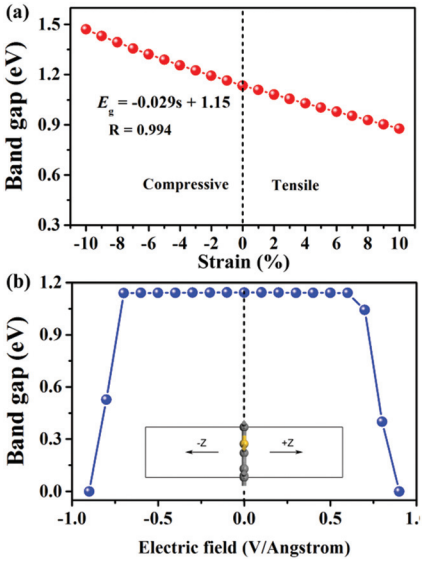

Fig. 4 (a) The electronic band gap of g-SiC_7 as a function of applied strain. Positive and negative values mean tensile and compressive strain, respectively. The red solid line represents the fitted linear relation in the form of $E_g = \alpha\sigma + \beta$, with $\alpha = -0.029$, $\beta = 1.15$. (b) The electronic band gap of g-SiC_7 under a perpendicular electric field that applies along both the $-Z$ and $+Z$ directions.

To make g-SiC_7 siligraphene more practical when applied in future electronic devices, we have investigated the modulation on the electronic band gap of g-SiC_7 by applying biaxial strain (σ) within the in-plane *x*- and *y*-direction simultaneously, or applying an external electric field perpendicular to the *xy* plane. The HSE06-calculated band gap of 1.13 eV is used as the neutral value when the applied strain is 0% or the external electric field strength is 0 V $Å^{-1}$. The corrected value is 0.36 eV (band gap difference between PBE and HSE06 results). As shown in Fig. 4a, a linear relationship between the applied biaxial strain and band gap is revealed. The linear fitting indicates that the band gap of g-SiC_7 is inversely proportional to the strain. Under the tensile strain, the band gap decreases with the increasing strain, while when applying the compressive strain, the band gap increases with the increasing strain. When the σ ranges from −10% to 10%, the band gap can be tuned in the range of 0.88–1.47 eV, which well satisfies the

demand of donor materials for solar cells with high energy-conversion efficiency.[39]

The variation of the band gap induced by the vertical electric field is also shown in Fig. 4b. As we can see, the orientation of the electric field has little influence on the band gap changing. It is obvious that the band gap of g-SiC_7 siligraphene is not sensitive to low electric field strength. However, when the electric field strength increases to 0.7 V $Å^{-1}$, the band gap dramatically decreases and leads to an electronic phase transition from a semiconductor to a conductor when the electric field strength is larger than 0.9 V $Å^{-1}$. It means that g-SiC_7 siligraphene works as a stable semiconductor when the external electric field strength is low ($\leq$0.7 V $Å^{-1}$) and can be rapidly converted to a conductor as soon as the field strength increases up to 0.9 V $Å^{-1}$. This special conversion between semiconductor and conductor points to the possibility of an all-electrical field controlled memory device based on g-SiC_7 siligraphene.[40]

We expect that incorporating silicon atoms into the graphene honeycomb lattice at a low concentration can improve graphene's light absorption efficiency and further extend graphene's application in photoelectronic devices. The direct band gap of 1.13 eV of g-SiC_7 siligraphene indicates a preferable efficiency of light absorption. Since DFT and HSE06 wrongly describe the reduced charge screening and the enhanced electron–electron correlation in the low-dimensional system, the GW calculations, as implemented in BerkeleyGW package,[41,42] were performed without self-consistency in the Green's function and the screened Coulomb interaction (G_0W_0 approximation) in combination with the random phase approximation (RPA) or Bethe–Salpeter equation (BSE) calculations to calculate the quasi-particle band gap and the light absorbance (A) with or without electron–hole (e–h) interactions. The g-SiC_7 siligraphene has an enlarged band gap of 1.55 eV, with a GW correction to the PBE band gap by about 0.79 eV. The light absorbance with electron–hole interaction obtained *via* GW plus Bethe–Salpeter equation (GW + BSE) is shown in Fig. 5. The first prominent peak corresponds to a bright exciton with an exciton binding energy of 0.55 eV, locating at 1.0 eV (defined as the optical band gap, E_g^{opt}), showing the most ideal optical band gap among the reported siligraphenes (Table 1). The exciton binding energies in g-SiC_2, g-SiC_7, and SL-SiC show a linear scaling as a function of the quasiparticle gap (see in Fig. S3†), in agreement with the previous finding in pure or chemical functionalized or strained 2D materials.[43] Compared with the widely investigated g-SiC_2 siligraphene and phosphorene,[44,45] g-SiC_7 siligraphene has an enhanced light absorbance with an average value beyond 10% of near infrared and visible photon energies in the 0.7–3.0 eV range of key relevance for photovoltaics. The superior light absorbance against the sunlight can be apparently inferred by the greater overlap with solar flux than phosphorene, as depicted in Fig. 5. The features above can also be quantified by the absorbed photon flux J_{abs}:

$$J_{abs} = e\int_{E_g^{opt}}^{\infty} A(\omega)J_{ph}(E)$$

Here $A(\omega)$is the monolayer absorbance of the 2D materials, whose calculation details can be found in the ESI.† $J_{ph}(E)$ is the incident photon flux (units of photons/(cm^2 s eV)), and E is the photon energy. J_{abs} is expressed as the equivalent short-circuit electrical current density (units of mA cm^{-2}) when every photon is converted to a carrier extracted in a solar cell, representing the upper limit for the contribution of the donor material to the short-circuit current in a solar cell.[46] The calculated J_{abs} in g-SiC_7 siligraphene is 4.64 mA cm^{-2}, obviously larger than that in g-SiC_2 siligraphene (4.06 mA cm^{-2}) and phosphorene (3.15 mA cm^{-2}),[47] and also larger than the reported graphene and transition metal dichalcogenide (TMD) monolayers (2–4.5 mA cm^{-2}).[46] The extraordinary sunlight adsorption performance suggests that g-SiC_7 siligraphene is a promising donor material for the photovoltaics applications.

In this article, the structure, stability, electronic and optical properties of the novel 2D nanomaterial g-SiC_7 siligraphene is systematically investigated by theoretical calculations. The g-SiC_7 siligraphene has a graphene-like honeycomb lattice and shows superior structural, dynamical and thermal stability. Unlike graphene, the g-SiC_7 siligraphene is a semiconductor with a direct band gap of 1.13 eV, which can be attributed to the broken conjugation system. Strain and vertical electric field both have good tunability of the band gap of g-SiC_7 siligraphene. Such a g-SiC_7 siligraphene shows superior sunlight optical absorbance, larger than g-SiC_2 siligraphene and single-layer black phosphorus (phosphorene) in near infrared and visible photon ranges, thus enabling it to be promising for applications in next-generation flexible optoelectronic devices as a donor material. And its sensitivity to a high-strength electrical field also makes it possible to function as an electrical field controlled memory device. These interesting results may stimulate further efforts on siligraphene based optoelectronic materials.

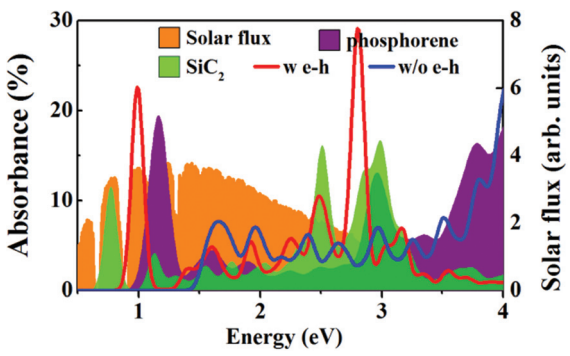

Fig. 5 The absorbance spectrum of g-SiC_7 siligraphene (with and without electron–hole interaction), g-SiC_2 siligraphene, as well as phosphorene (along the armchair direction), overlapped to the incident AM1.5 G solar flux.

Acknowledgements

The work is supported by the National Basic Research Program of China (973 Program, Grant No. 2012CB932400), the National Natural Science Foundation of China (Grant No. 21273158), a Project Funded by the Priority Academic Program Development of Jiangsu Higher Education Institutions (PAPD). This is also a project supported by the Fund for Innovative Research Teams of Jiangsu Higher Education Institutions, the Jiangsu Key Laboratory for Carbon-Based Functional Materials and Devices, the Collaborative Innovation Center of Suzhou Nano Science and Technology. L. Z. acknowledges financial support from the Bremen TRAC–COFUND fellowships, co-financed by the Marie Curie Program of the European Union. The support of the Supercomputer Center of Northern Germany (HLRN Grant No. hbp00027) is also acknowledged.

References

1 X. Wan, Y. Huang and Y. Chen, *Acc. Chem. Res.*, 2012, **45**, 598–607.
2 A. K. Geim and K. S. Novoselov, *Nat. Mater.*, 2007, **6**, 183–191.
3 V. Barone, O. Hod and G. E. Scuseria, *Nano Lett.*, 2006, **6**, 2748–2754.
4 S. Zhou, G.-H. Gweon, A. Fedorov, P. First, W. De Heer, D.-H. Lee, F. Guinea, A. C. Neto and A. Lanzara, *Nat. Mater.*, 2007, **6**, 770–775.
5 M. Yankowitz, J. Xue, D. Cormode, J. D. Sanchez-Yamagishi, K. Watanabe, T. Taniguchi, P. Jarillo-Herrero, P. Jacquod and B. J. LeRoy, *Nat. Phys.*, 2012, **8**, 382–386.
6 G. Lu, K. Yu, Z. Wen and J. Chen, *Nanoscale*, 2013, **5**, 1353–1368.
7 L.-J. Zhou, Y.-F. Zhang and L.-M. Wu, *Nano Lett.*, 2013, **13**, 5431–5436.
8 J. Hackley, D. Ali, J. DiPasquale, J. Demaree and C. Richardson, *Appl. Phys. Lett.*, 2009, **95**, 133114.
9 J. Moon, D. Curtis, S. Bui, T. Marshall, D. Wheeler, I. Valles, S. Kim, E. Wang, X. Weng and M. Fanton, *IEEE Electron Device Lett.*, 2010, **31**, 1193–1195.
10 Y. Xu, K. He, S. Schmucker, Z. Guo, J. Koepke, J. Wood, J. Lyding and N. Aluru, *Nano Lett.*, 2011, **11**, 2735–2742.
11 C. Tayran, Z. Zhu, M. Baldoni, D. Selli, G. Seifert and D. Tománek, *Phys. Rev. Lett.*, 2013, **110**, 176805.
12 X. Dang, H. Dong, L. Wang, Y. Zhao, Z. Guo, T. Hou, Y. Li and S.-T. Lee, *ACS Nano*, 2015, **9**, 8562–8568.
13 X. Lin, S. Lin, Y. Xu, A. A. Hakro, T. Hasan, B. Zhang, B. Yu, J. Luo, E. Li and H. Chen, *J. Mater. Chem. C*, 2013, **1**, 2131–2135.
14 S. Lin, *J. Phys. Chem. C*, 2012, **116**, 3951–3955.
15 Y. Li, F. Li, Z. Zhou and Z. Chen, *J. Am. Chem. Soc.*, 2010, **133**, 900–908.
16 P. Li, R. Zhou and X. C. Zeng, *Nanoscale*, 2014, **6**, 11685–11691.
17 Y. Ding and Y. Wang, *J. Phys. Chem. C*, 2014, **118**, 4509–4515.
18 Z. Shi, Z. Zhang, A. Kutana and B. I. Yakobson, *ACS Nano*, 2015, **9**, 9802–9805.
19 J. Zhang, J. Ren, H. Fu, Z. Ding, H. Li and S. Meng, *Sci. China: Phys., Mech. Astron.*, 2015, **58**, 1–8.
20 S. Lin, S. Zhang, X. Li, W. Xu, X. Pi, X. Liu, F.-C. Wang, H.-A. Wu and H. Chen, *J. Phys. Chem. C*, 2015, **119**, 19772–19779.
21 M. Zhao and R. Zhang, *Phys. Rev. B: Condens. Matter*, 2014, **89**, 195427.
22 H. Dong, B. Lin, K. Gilmore, T. Hou, S.-T. Lee and Y. Li, *J. Power Sources*, 2015, **299**, 371–379.
23 G. Kresse and J. Furthmüller, *Phys. Rev. B: Condens. Matter*, 1996, **54**, 11169–11186.
24 G. Kresse and J. Hafner, *Phys. Rev. B: Condens. Matter*, 1993, **48**, 13115–13118.
25 G. Kresse and D. Joubert, *Phys. Rev. B: Condens. Matter*, 1999, **59**, 1758–1775.
26 J. P. Perdew, K. Burke and M. Ernzerhof, *Phys. Rev. Lett.*, 1996, **77**, 3865–3868.
27 G.-B. Liu, D. Xiao, Y. Yao, X. Xu and W. Yao, *Chem. Soc. Rev.*, 2015, **44**, 2643–2663.
28 J. Heyd, G. E. Scuseria and M. Ernzerhof, *J. Chem. Phys.*, 2003, **118**, 8207–8215.
29 J. Heyd, G. E. Scuseria and M. Ernzerhof, *J. Chem. Phys.*, 2006, **124**, 219906.
30 R. F. Bader, *Atoms in Molecules: A Quantum Theory*, Oxford University Press, Oxford, 1990.
31 G. Henkelman, A. Arnaldsson and H. Jónsson, *Comput. Mater. Sci.*, 2006, **36**, 354–360.
32 M. Menon, E. Richter, A. Mavrandonakis, G. Froudakis and A. N. Andriotis, *Phys. Rev. B: Condens. Matter*, 2004, **69**, 115322.
33 M. Zhao, Y. Xia, F. Li, R. Zhang and S.-T. Lee, *Phys. Rev. B: Condens. Matter*, 2005, **71**, 085312.
34 K. M. Alam and A. K. Ray, *Phys. Rev. B: Condens. Matter*, 2008, **77**, 035436.
35 T. Taguchi, N. Igawa, H. Yamamoto and S. Jitsukawa, *J. Am. Ceram. Soc.*, 2005, **88**, 459–461.
36 L. Pei, Y. Tang, Y. Chen, C. Guo, X. Li, Y. Yuan and Y. Zhang, *J. Appl. Phys.*, 2006, **99**, 114306.
37 H. C. Hsueh, G. Y. Guo and S. G. Louie, *Phys. Rev. B: Condens. Matter*, 2011, **84**, 085404.
38 A. Fleurence, R. Friedlein, T. Ozaki, H. Kawai, Y. Wang and Y. Yamada-Takamura, *Phys. Rev. Lett.*, 2012, **108**, 245501.
39 M. C. Scharber, D. Muhlbacher, M. Koppe, P. Denk, C. Waldauf, A. J. Heeger and C. J. Brabec, *Adv. Mater.*, 2006, **18**, 789.
40 Q. F. Gu, J. H. He, D. Y. Chen, H. L. Dong, Y. Y. Li, H. Li, Q. F. Xu and J. M. Lu, *Adv. Mater.*, 2015, **27**, 5968–5973.
41 M. Rohlfing and S. G. Louie, *Phys. Rev. B: Condens. Matter*, 2000, **62**, 4927–4944.

42 J. Deslippe, G. Samsonidze, D. A. Strubbe, M. Jain, M. L. Cohen and S. G. Louie, *Comput. Phys. Commun.*, 2012, **183**, 1269–1289.
43 J.-H. Choi, P. Cui, H. Lan and Z. Zhang, *Phys. Rev. Lett.*, 2015, **115**, 066403.
44 L. Kou, C. Chen and S. C. Smith, *J. Phys. Chem. Lett.*, 2015, **6**, 2794–2805.
45 H. Liu, A. T. Neal, Z. Zhu, Z. Luo, X. Xu, D. Tománek and P. D. Ye, *ACS Nano*, 2014, **8**, 4033–4041.
46 M. Bernardi, M. Palummo and J. C. Grossman, *Nano Lett.*, 2013, **13**, 3664–3670.
47 L. Zhou, J. Zhang, Z. Zhuo, L. Kou, W. Ma, B. Shao, A. Du, S. Meng and T. Frauenheim, 2015, *arXiv:1512.01675 [cond-mat.mtrl-sci]*.